


RESEARCH

Open Access



A patient-derived organoid-based study identified an ASO targeting SNORD14E for endometrial cancer through reducing aberrant FOXM1 Expression and β -catenin nuclear accumulation

Xi Chen¹, Xin Liu¹, Qian-hui Li¹, Bing-feng Lu¹, Bu-min Xie¹, Yu-meng Ji¹ and Yang Zhao^{1*} 

Abstract

Background Most of the endometrial cancer (EC) patients are diagnosis in early stage with a good prognosis while the patients with locally advanced recurrent or metastatic result in a poor prognosis. Adjuvant therapy could benefit the prognosis of patients with high-risk factors. Unfortunately, the molecular classification of great prognostic value has not yet reached an agreement and need to be further refined. The present study aims to identify new targets that have prognostic value in EC based on the method of EC patient-derived organ-like organs (PDOs), and further investigate their efficacy and mechanism.

Methods The Cancer Genome Atlas (TCGA) database was used to determine SNORD14E expression. The effects of SNORD14E were investigated using CCK8, Transwell, wound-healing assays, and a xenograft model experiment; apoptosis was measured by flow cytometry. Antisense oligonucleotide (ASO) targeting SNORD14E was designed and patient-derived organoids (PDO) models in EC patients was established. A xenograft mouse and PDO model were employed to evaluate the effects of ASO targeting SNORD14E. RNA-seq, Nm-seq, and RNA immunoprecipitation (RIP) experiments were employed to confirm the alternative splicing (AS) and modification induced by SNORD14E. A minigene reporter gene assay was conducted to confirm AS and splicing factors on a variable exon. Actinomycin-D (Act-D) and Reverse Transcription at Low deoxy-ribonucleoside triphosphate concentrations followed by PCR (RTL-P) were utilized to confirm the effects of 2'-O methylation modification on FOXM1.

Results We found that SNORD14E was overexpressed in EC tissues and patients with high expressed SNORD14E were distributed in the TCGA biomolecular classification subgroups without difference. Further, SNORD14E could reduce disease-free survival (DFS) and recurrence free survival (RFS) of EC patients. SNORD14E promoted proliferation, migration, and invasion and inhibited the apoptosis of EC cells in vitro. ASOs targeting SNORD14E inhibited cell proliferation, migration, invasion while promoted cell apoptosis. ASOs targeting SNORD14E inhibited tumor growth in the xenograft mouse model. TCGA-UCEC database showed that the proportion of patients with high expression of SNORD14E in middle-high risk and high-risk patients recommended by EMSO-ESGO-ESTRO guidelines for adjuvant therapy is more than 50%. Next, we enrolled 8 cases of high-risk and high-risk EC patients according

*Correspondence:

Yang Zhao

yida.zhaoyang@163.com

Full list of author information is available at the end of the article



© The Author(s) 2023. **Open Access** This article is licensed under a Creative Commons Attribution 4.0 International License, which permits use, sharing, adaptation, distribution and reproduction in any medium or format, as long as you give appropriate credit to the original author(s) and the source, provide a link to the Creative Commons licence, and indicate if changes were made. The images or other third party material in this article are included in the article's Creative Commons licence, unless indicated otherwise in a credit line to the material. If material is not included in the article's Creative Commons licence and your intended use is not permitted by statutory regulation or exceeds the permitted use, you will need to obtain permission directly from the copyright holder. To view a copy of this licence, visit <http://creativecommons.org/licenses/by/4.0/>. The Creative Commons Public Domain Dedication waiver (<http://creativecommons.org/publicdomain/zero/1.0/>) applies to the data made available in this article, unless otherwise stated in a credit line to the data.

to EMSO-ESGO-ESTRO guidelines and successfully constructed EC-PDOs. ASOs targeting SNORD14E inhibited the EC-PDO growth. Mechanistically, SNORD14E could recognize the mRNA of FOXM1 and recruit SRSF1 to promote the shearing of the variable exon VIIa of FOXM1, resulting in the overexpression of the FOXM1 malignant subtypes FOXM1b and FOXM1c. In addition, SNORD14E modified FOXM1 mRNA with 2'-O-methylation, which prolonged the half-life of FOXM1 mRNA. The nucleus accumulation of β -catenin caused by aberrant FOXM1 expression led to EC progression.

Conclusions ASO targeting SNORD14E can be an effective treatment for EC.

Keywords Endometrial cancer, Patients-derived organoid, ASO targeted therapy, Alternative splicing, 2'-O-methylation modification

Background

Endometrial cancer (EC) is one of the most common gynecological malignancy in women. Most of the EC patients were diagnosed in the early stage. About 80% patients with early EC had a good prognosis, and the 5-year overall survival rate was 95% [1, 2]. The prognosis of patients with advanced and recurrent EC is poor (5-year survival rate < 20%) [3]. Although the risk of recurrence of early EC after initial treatment is low (7.2%), about 15–20% EC patients may have a high risk of advanced disease or disease recurrence, and the recurrence rate is close to 20–25% [4, 5]. Identifying and giving high-risk patients the best adjuvant therapy to improve their prognosis is still the biggest challenge of EC treatment.

In 2013, TCGA first proposed four distinct molecular classification based on the molecular characterization of EC [6]. Recently, new molecular classification methods such as ProMisE, TransPORTEC and Parra-Herran have been proposed due to the complicated and poor in clinical translation of the original TCGA molecular classification. At present, all biomolecular classification methods still have inevitable errors, and no consistent conclusion has been reached so far [7–9].

The ESMO-ESGO-ESTRO guidelines recommend adjuvant therapy for patients in middle-high risk group and high-risk group to improve prognosis [3]. We take snoRNA as the research target and analyze the TCGA-UCEC database. We have found that SNORD14E was aberrantly expressed in EC tissues and reduce DFS and RFS of patients with EC. The patients with high expressed SNORD14E were distributed in the TCGA biomolecular classification subgroups without difference. The results suggested that SNORD14E could be a target that can affect the prognosis of EC patients independent of biomolecular classification. We further grouped the EC patients in TCGA database based on the ESMO-ESGO-ESTRO risk classification, and found that patients with high level of SNORD14E were widely presented in all risk subgroup. Notably, the proportion

of patients with high level of SNORD14E in the middle-high risk group and high-risk group which recommended by the guidelines for adjuvant therapy are over 50%. This suggested that the treatment targeting SNORD14E may bring benefits to the prognosis of nearly 50% patients in the middle-high risk group and high-risk group. The following in vitro experiments in EC cells showed that SNORD14E promoted proliferation, migration, and invasion and inhibited the apoptosis. ASOs targeting SNORD14E inhibited cell proliferation, migration, invasion while promoted cell apoptosis. ASOs targeting SNORD14E inhibited tumor growth in the xenograft mouse model.

Due to the complexity of human tumors, the response to clinical cancer treatments varies substantially. Recently, organoid culture technologies have been developed, including EC tissues [10]. Patient-derived organoids (PDOs) maintains pathological and molecular properties of EC with great experimental accessibility and lower cost than animal models. Additionally, PDOs are considered to better represent the natural state of the tumor than cell lines and therefore serves as the suitable models for potential treatment reagents. In order to further explore the therapeutic effect of ASO targeting SNORD14E, we constructed 8 EC-PDO models from patients with high level of SNORD14E in middle-high risk or high-risk group, and found that ASO-SNORD14E can inhibit the proliferation of the 8 EC-PDOs. In this study, we have identified a snoRNA, SNORD14E, which plays an oncogenic role in EC via two distinct mechanisms to induce β -catenin nuclear accumulation through FOXM1. The therapeutic value of the targeted drug ASO-SNORD14E was verified at multiple levels, including the EC-PDOs. We have further investigated the molecular mechanism of malignant biological behavior in EC caused by SNORD14E, and the potential of SNORD14E as a therapeutic target to improve the prognosis of patients with EC, especially those in middle-high risk and high-risk group.

Methods

Study design

The study is a preclinical study which aims to assess the therapeutic effect of the ASO-SNORD14E in EC patients at multiple levels. The participants were required to provide written informed consent before participating in the study. The study protocol was approved by the Ethics Committee of Guangzhou Medical University (2020066). Patients received standard treatment according to clinical treatment guidelines, and patient tissues obtained from surgery were used to construct PDO and evaluate the responsiveness to ASO (Fig. 8F).

Setting and participants

Participants were adults (age ≥ 18 years old) histologically confirmed EC, and none of the enrolled patients received anti-tumor related treatment. The participants were all from patients with EC who underwent surgery in the Third Affiliated Hospital of Guangzhou Medical University from April 22, 2022 to March 30, 2023. And all the patients were operable endometrial cancer patients. Risk classification is carried out according to ESMO-ESGO-ESTRO guideline. The expression of SNORD14E of EC patients in middle-high risk group and high-risk group was detected, and patients with high expression of SNORD14E were selected for EC-PDO construction and ASO treatment (Fig. 8G, Supplementary Table 4). The 8 patients enrolled in the study were all survival without recurrence due to the short postoperative time.

Variables

In the study, self-control was adopted to minimize confounder factors as EC-PDOs were from tissues of EC patients. EC-PDOs from the same EC patient tissue were randomly grouped and treated with ASO drugs or untreated. The changes of EC-PDO volume were counted respectively, and the proliferation of PDO was measured by CellCounting-Lite 3D luminescent cell vitality.

Bias

Firstly, considering the selection bias and confounder bias caused by the difference of individual responses to drugs, we have PDOs from the same patient were randomly divided into experimental group and control group for treatment respectively. Secondly, in order to avoid the selection bias caused by the PDO initial volume, PDOs with the initial diameter limit of 50–150 μm [11] were selected for tracking and statistical analysis. Thirdly, there may be information bias caused by the

difference between the actual size of PDO and the measured value due to the irregular shape of PDOs. We use the change of PDO area to measure the effect of ASO drugs on PDO proliferation. Fourth, different researchers are responsible for grouping and measurement separately to collect data blindly to limit information bias. Finally, in order to avoid the confounder bias caused by pollution, growth environment differences and other factors, medium both of the experimental group and the control group were changed and added at the same time during the treatment, and keeping asepsis.

Study size

Eight samples that can meet the enrollment criteria were included in the study to construct PDO. The PDOs with appropriate size (diameter 50–150 μm) were selected for statistical analysis to avoid the influence of PDO initial volume. In the eight cases of EC-PDO, no less than 5 PDOs of each case were included in each group for measurement, and the data conform to normal distribution and statistically analyzed by paired *t*-test.

PDO models and ASO treatment

The generation of EC organoids was performed as described previously [12]. Briefly, EC tissues were cut into 1–3-mm³ pieces and digested for 15 min in TrypLE (12604013, Thermo Fisher Scientific). The organoid was suspended with 40% complete medium [13] and 60% Matrigel mixture. Then, 20- μL droplets were deposited in prewarmed 48-well plates (Corning dishes). Passaging was performed every 10–15 days.

For transfection-free uptake in ASO treatment, 8 nM SNORD14E-specific ASO or ASO-NC was added into medium (Supplementary Table 3). An organoid and ASO were co-incubated for 7 or 9 days. For visualization of organoid proliferation, images were obtained using an inverted microscope (Nikon) at 4 \times magnification.

Organoid lentiviral transduction

Organoids were digested and resuspended in a medium. Cells were spin-infected (700 g, 90 min, 25 °C) on low-adhesion plates (Corning), and incubated at 37 °C for 4–5 h. The organoids were then centrifuged at 300 g for 3 min at 4 °C and seeded in Matrigel.

PDO viability assay

The viability of organoids was measured following the methods of CellCounting-Lite 3D Luminescent Cell Viability Assay (Vazyme, DD1102-01). Briefly, organoids were digested and seeded into 96-well plates. Each plate was placed at room temperature for 30 min before adding an equal volume of CellCounting-Lite 3D, followed

by vigorous shaking for 5 min to lyse the cell mass fully. Plates were incubated at 25 °C for 25 min and the fluorescence intensity was detected.

Human EC xenograft tumor models and treatment

All animal experiments were approved by the Animal Experimental Ethics Committee of Guangdong Medical Laboratory Animal Center. Briefly, 1×10^6 HEC-1B cells and 2×10^6 Ishikawa cells were injected subcutaneously into 4–6-week-old female nude mice. The tumor were monitored every three days for 40 days. After successful formation, tumors were collected for further IHC staining. Tumor volumes were measured and calculated as: Tumor volume (mm^3) = $0.5 \times \text{length} \times \text{width}^2$. Tumor diameters were measured with a Vernier caliper.

ASO treatment of the xenograft tumor was initiated after the tumor volume reached 50mm^3 . Mice were randomized (five mice with HEC-1B cells per group and four mice with Ishikawa cells per group), and ASO-NC (8 nM) and ASO-SNORD14E (8 nM) were separately injected into tumors. The diameters of the tumors were monitored every three days, and the mice were sacrificed approximately 40 days after cell injection.

Immunohistochemistry (IHC) and immunofluorescence (IF) assays

Tissues were fixed with 4% paraformaldehyde at 4 °C, while PDOs were fixed with 4% paraformaldehyde at room temperature for 15 min. Samples were embedded in paraffin. Then, the 5- μm -thick slices were subjected to IHC or IF assays. The antibodies used for staining were: ER (Proteintech, 21244–1-AP), PR (Proteintech, 25871–1-AP), and Ki67 (Proteintech, 27309–1-AP), FOXM1 (Proteintech, 13147–1-AP).

Cell culture

The human EC cell lines HEC-1A, HEC-1B, Ishikawa, and KLE were purchased from the American Type Culture Collection (ATCC), and the hESC, hEEC and 293 T cell lines were obtained from Guangzhou Jennio Biotech Co., Ltd (Guangzhou, China). Cells were cultured by Dulbecco's Modified Eagle Medium (HEC-1B) or RPMI 1640 medium (Ishikawa) with 10% FBS and 1% penicillin/streptomycin.

Cell proliferation, migration, and invasion assays

Cell growth was detected using CCK-8 assays. The ability of migration and invasion were assessed by scratch assays and Transwell invasion assays as earlier reported [14].

RNA-seq and Nm-seq

HEC-1B cells transfected with vector or SNORD14E plasmids were harvested. Total RNA was obtained using

TRIzol reagent (Takara) as described before and sent for sequencing. NM-Seq service was provided by CloudSeq Biotech Inc. (Shanghai, China) by following the published procedures [15]. Libraries were constructed using NEBNext Small RNA Library Prep Set for Illumina (New England BioLabs). Sequencing was then performed on Illumina HiSeq4000 according to the manufacturer's instructions.

Reverse transcription-polymerase chain reaction (RT-PCR) analysis of splicing isoforms

Total RNA was isolated using the TRIzol reagent (Takara) following the standard protocol. qRT-PCR was performed according to the instructions of Hieff[®] qPCR SYBR Green Master Mix (High Rox Plus) (Yeasen, Shanghai, China). The RNA changes were calculated by the $2^{-\Delta\Delta\text{Ct}}$ method. Primers were synthesized by BGI company (Shenzhen, China) (Supplementary Table 1).

RNA Immunoprecipitation (RIP)

Briefly, cells were lysed with RIP lysis buffer containing an RNA inhibitor and protease. The supernatant of the cell lysate was collected and incubated with antibody-conjugated beads at 4 °C overnight. The binding complexes were washed, purified, and analyzed by qRT-PCR.

Minigene assay

FOXM1 minigene plasmids were constructed based on the genomic sequence spanning exons VIIa of the human FOXM1 gene and cloning it into the GV658 vector. Mutants with a specific sequence deletion were created based on the primary minigene.

Nuclear-cytoplasmic fractionation

To perform subcellular fractionation of RNA and protein, we followed the instructions on the Nuclear and Cytoplasmic Protein Extraction Kit (Beyotime, P0028). Then, we added 1 mM PMSF (Beyotime, ST506) to the nuclear and cytoplasmic fractions. RNA was extracted using the TRIzol protocol (Takara, 9108). Protein was collected and target protein was detected with western-blot.

Western-blot analysis

Proteins were extracted with RIPA lysate (#P0013B, Beyotime, Shanghai, China) or Nuclear and Cytoplasmic Protein Extraction Kit (Beyotime, P0028) and measured using BCA protein assay kit (#P0009, Beyotime, Shanghai, China). Protein (30 μg) was pipetted into SDS-PAGE gel and transferred to PVDF membrane. Membranes were blocked and incubated with primary and secondary antibodies. Imaging was performed using BeyoECL Star (#P0018AM, Beyotime, Shanghai, China).

RTL-P assay for RNA 2'-O-methylation

100 ng of total RNA was used for RT reacted in 25- μ L reaction cocktails with and 50 μ M of specific RT primers (Supplementary Table 2) that were denatured at 70 °C for 10 min, and then placed on ice. The RT buffer containing 200 U M-MLV reverse transcriptase (Takara), 40 U RNasin Ribonuclease inhibitor (Takara), and a low (10 μ M) or high (1 mM) concentration of dNTPs were employed for an initial annealing step at 42 °C for 1 h and heated at 70 °C for 15 min. Then, the PCR reaction was terminated.

RNA stability assay

EC cells were transfected with SNORD14E or a vector and treated with actinomycin D (ActD, S8964, Selleck) at a final concentration of 50 μ g/mL for 2, 4, 6, 8, and 10 h. Total RNA was extracted and analyzed by qRT-PCR. Then, a calculation of the RNA half-life of SNORD14E was performed.

Statistical analysis

GraphPad Prism 8.0 (La Jolla, CA, USA) was employed for statistical analyses and ImageJ measures PDO area. Volcano plot was plotted by <https://www.bioinformatics.com.cn>, an online platform for data analysis and visualization. All experiments were performed at least three times. For two-group comparisons, we employed the *t*-test, whereas one- or two-way ANOVA was conducted for multiple comparisons with 95% confidence intervals. $P < 0.05$ (*), $P < 0.01$ (**), and $P < 0.001$ (***)

Results

SNORD14E is overexpressed in endometrial carcinoma and is associated with poor prognosis

To investigate the role of SNORD14E in EC, we analyzed a UCEC dataset from The Cancer Genome Atlas (TCGA, <http://cancergenome.nih.gov>) and found that SNORD14E was upregulated in EC (Fig. 1A). The characteristics of patients with EC were collected from TCGA database. The patients were divided into two groups (high vs. low) based on the the optimal critical value of SNORD14E in TCGA-UCEC selected by Kaplan–Meier, a prognostic analysis website (<http://kmplot.com/analysis/>) [16]. It showed that patients with high expressed SNORD14E were distributed in the TCGA biomolecular classification subgroups without difference, and the overexpression of SNORD14E was correlated with reduced DFS and RFS (Fig. 1B). The prognosis risk group of TCGA-UCEC patients according to ESMO-ESGO-ESTRO risk classification showed that the proportion of patients with high level of SNORD14E in the middle-high risk group and the high-risk group was more than 50%.

Finally, we examined SNORD14E expression in EC cell lines, which included HEC-1A, HEC-1B, KLE, Ishikawa,

and normal endometrial cell lines hEEC and hESC. Our results showed that SNORD14E was more upregulated in EC cells than in normal endometrial cell lines (Fig. 1C). Nuclear/cytoplasm fractionation analysis revealed that SNORD14E was located in both the cytoplasm and the nucleus (Fig. 1D). These data suggest that SNORD14E may be involved in EC progression.

SNORD14E promotes malignant biological behavior of EC cells in vitro and in vivo

Considering that SNORD14E is potentially involved in EC progression, we constructed SNORD14E-expressing plasmids and transfected them into Ishikawa and HEC-1B cell lines (Fig. 2A). Our results showed that SNORD14E promoted cell proliferation (Fig. 2B). Less apoptosis was observed in cells with upregulated SNORD14E (Fig. 2C). Compared with the control group, SNORD14E significantly promoted cell migration and invasion (Fig. 2D–E). Collectively, SNORD14E plays a crucial role in EC in vitro.

SNORD14E recruits SRSF1 and affects FOXM1 alternative splicing

To establish the mechanisms by which SNORD14E promotes EC progression, we conducted RNA-seq of HEC-1B cells with and without SNORD14E overexpression. The differentially expressed genes heatmaps and volcano plots are represented in Fig. 3A–B. Interestingly, differential AS events occurred after SNORD14E overexpression, including 852 skipped exons (Fig. 3C). We identified 122 genes that were differentially expressed in TCGA-UCEC and involved in the differential AS events. Additionally, 28 critical genes were identified to be both differentially expressed in TCGA UCEC and involved in skipped exon events after SNORD14E overexpression (Fig. 3D).

Studies have shown that over 300 splicing factors can regulate AS [17–19]. Therefore, we performed a RIP-PCR assay using the splicing factors that had been previously investigated and found to act as oncogenes in cancer development. We examined SF3B1, U2AF1, and SRSF1, and found that SNORD14E was enriched in the serine and arginine-rich splicing factor 1 (SRSF1) (Fig. 3E). As a member of the serine/arginine (SR) protein family of splicing activators, SRSF1 plays a role in exon definition and exerts exons splicing activation by binding directly to pre-mRNA [19]. After the snoRNA and RNA binding protein form a complex (snoRNPs), biological processes required a directly binding through base-pair interaction between the pre-mRNA and the RNA component of the snoRNP [20]. Next, we investigated the genes with potential SNORD14E-binding sites (IntaRNA program (<http://rna.informatik.uni-freiburg.de>)) and found three genes (Supplementary Figure A). Subsequently, RIP-PCR was

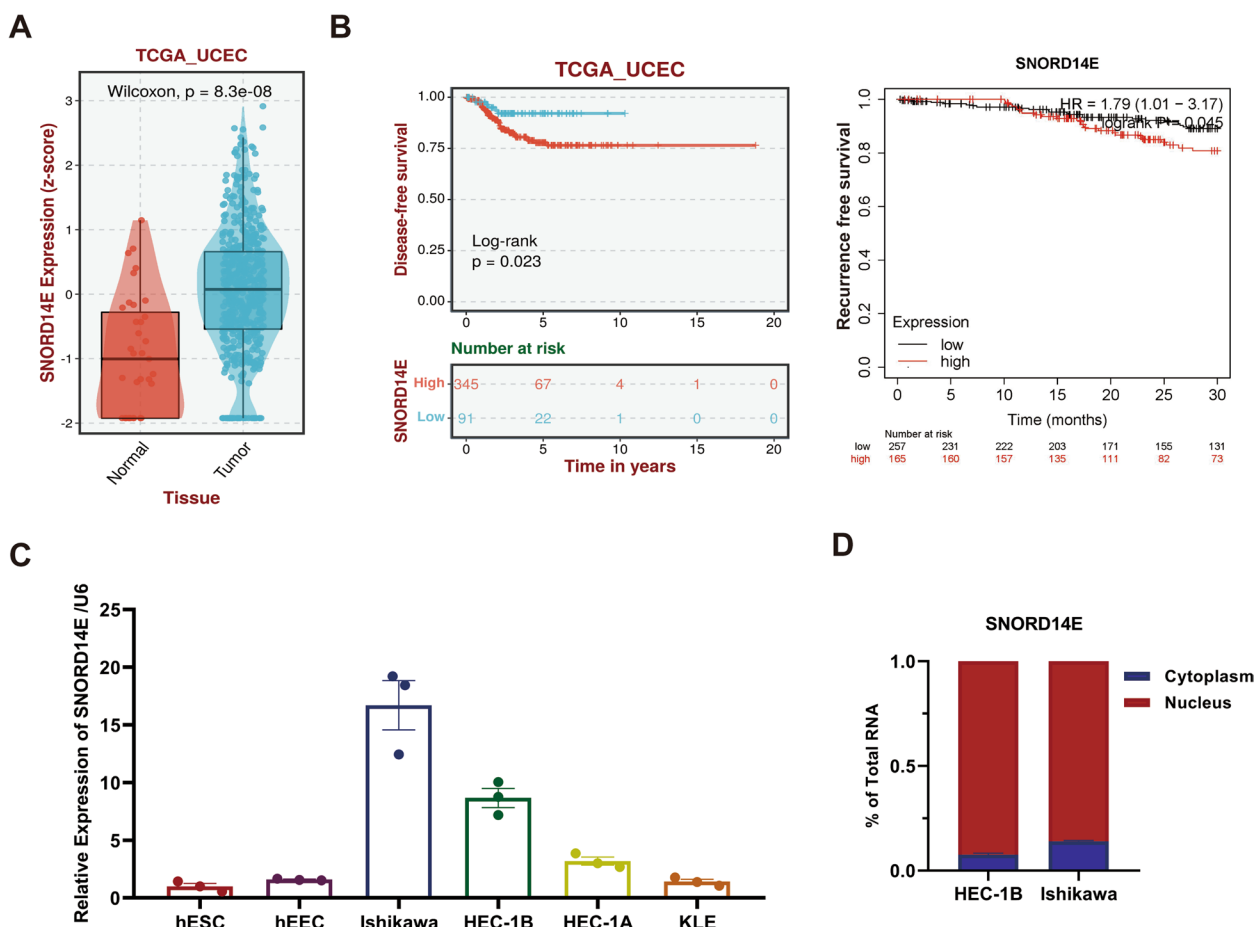


Fig. 1 SNORD14E is overexpressed in endometrial carcinoma and is associated with poor prognosis. **A** The expression of SNORD14E in normal endometrial tissue and in endometrial cancer tissue from the TCGA dataset. **B** Kaplan–Meier analysis of Disease-free survival ($P=0.023$, log-rank test) and Recurrence free survival ($P=0.045$) of EC patients with low or high SNORD14E expression according to the TCGA dataset. **C** The relative expression level of SNORD14E in EC cell lines, including HEC-1A, HEC-1B, Ishikawa and KLE examined by Real-time RT-PCR, compared to normal human endometrium cell line: hESC and hEEC. **D** SNORD14E was majorly localized in the nuclear of HEC-1B cells using nuclear and cytoplasmic RNA fractionation assay followed by Real-time RT-PCR

employed to detect the mRNA enriched in SRSF1, and finally, we obtained FOXM1 (Fig. 3F, Supplementary Figure B).

SRSF1 recruited by SNORD14E recognizes exonic splicing enhancers (ESEs) on VIIa and affects FOXM1 alternative splicing

FOXM1 consists of ten exons, including exons I-VIII and two alternatively spliced exons (Va, VIIa). Depending on the alternative exons Va and VIIa, three main FOXM1 isoforms can be identified: FOXM1a that includes ten exons, FOXM1b is lacking alternative exons Va and VIIa, and FOXM1c that includes Va but lacks VIIa (Fig. 4A). We constructed primers to determine the abnormal skipped exon of FOXM1 caused by SNORD14E. Then, we amplified all isoforms retaining or skipping the two alternative exons using the primers we designed. As

expected, FOXM1 had abnormally skipped exon VIIa in SNORD14E-overexpressing cells, which increased the content of FOXM1b and FOXM1c (Fig. 4B).

Exonic splicing enhancers (ESEs) are binding elements for specific SR proteins which are prevalent and could promote exon definition by directly recruiting the splicing machinery through their RS domain [21–23]. ESE Finder (<http://exon.cshl.edu/ESE/>) was employed for the prediction of ESEs on VIIa. Two potential ESE elements on VIIa were detected that could bind to SRSF1 (Fig. 4C). Notably, knockdown of SRSF1 significantly inhibited the skipping of FOXM1 VIIa, indicating that the skipping of FOXM1 VIIa was SRSF1-dependent (Fig. 4D).

To obtain more mechanistic insights into SRSF1 regulation of FOXM1 VIIa skipping, a minigene reporter plasmid (FOXM1-FL) was constructed, which was composed of a genomic DNA fragment of the FOXM1 exons

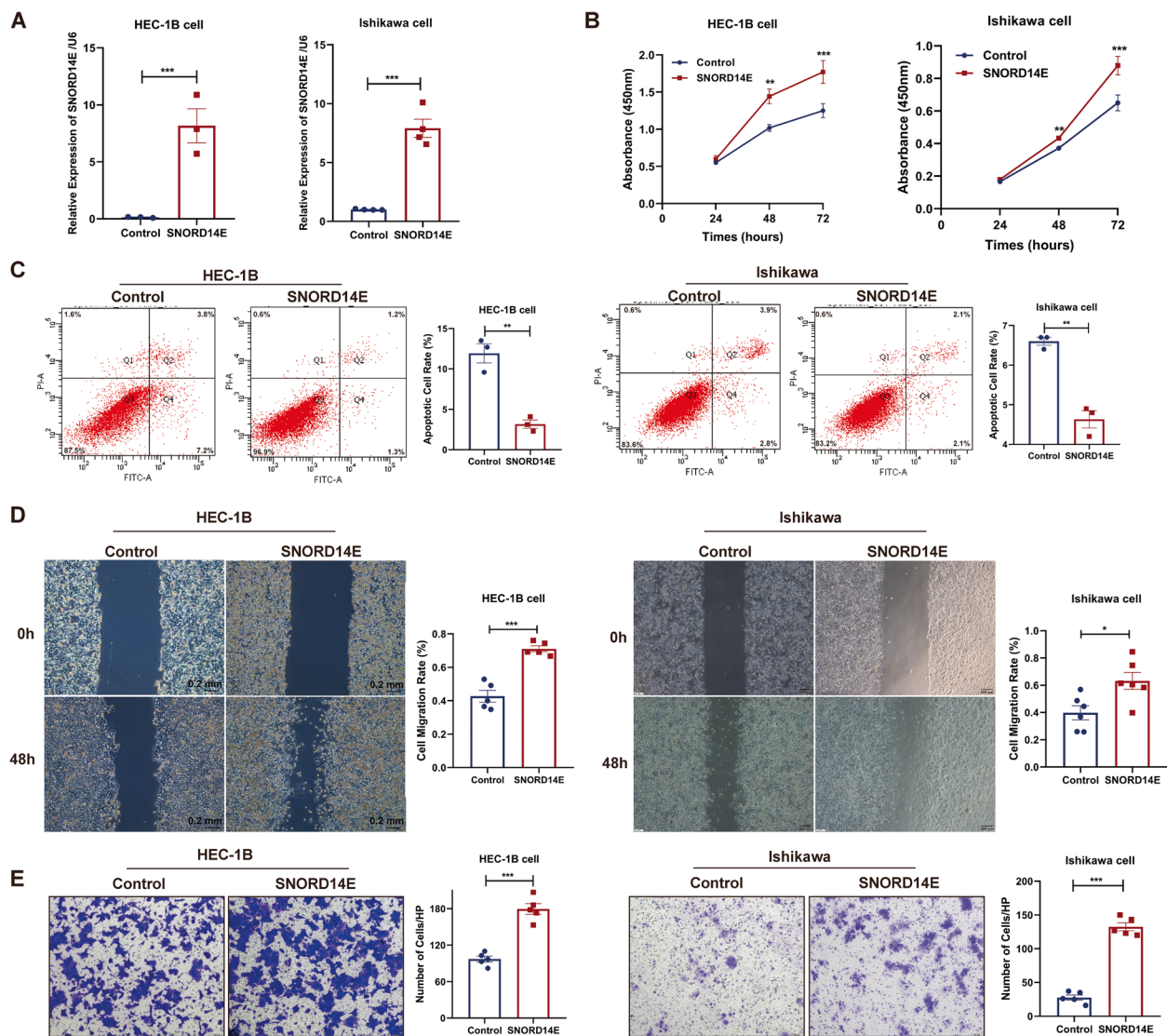


Fig. 2 SNORD14E promotes malignant biological behavior of endometrial carcinoma cells in vitro and in vivo. **A** RT-PCR analysis was performed to detect the RNA levels of SNORD14E in HEC-1B and Ishikawa cells with or without SNORD14E stable overexpression. **B** Cell proliferation assays of HEC-1B and Ishikawa cells with or without SNORD14E overexpression. **C** Flow apoptosis was performed to analyze cell apoptosis caused by SNORD14E overexpression. Wound healing and Transwell assays (**D-E**) were employed for detecting cell migration and invasion caused by SNORD14E. * $P < 0.05$, ** $P < 0.01$, *** $P < 0.001$

VII, VIIa, and VIII and 300 bp sequences at each end of introns. Next, we generated fragment deletion mutation plasmids in which the potential ESEs of exon VIIa were respectively deleted (FOXM1-del1 and FOXM1-del2) based on the FOXM1-FL minigene to explore the function of these ESEs in FOXM1 VIIa skipping (Fig. 4E). FOXM1-del1 and FOXM1-del2 showed lower exon VIIa skipped effects than FOXM1-FL in FOXM1 VIIa skipping (Fig. 4F). Altogether, these results suggested that the selected ESEs could all be recognized by SRSF1, and the recognition might be affected by SNORD14E.

Enrichment of the SRSF1-binding motif within FOXM1 VIIa resulted in FOXM1 VIIa skipping, a process that SNORD14E was able to facilitate by recruiting SRSF1.

SNORD14E induces β -catenin nuclear accumulation and facilitates EC progression through FOXM1 VIIa skipping

Next, we constructed a siRNA targeting FOXM1 or SRSF1 and determined its inhibitory efficiency (Fig. 5A). The siRNA was transfected into SNORD14E-overexpressing cells, which inhibited EC cell proliferation

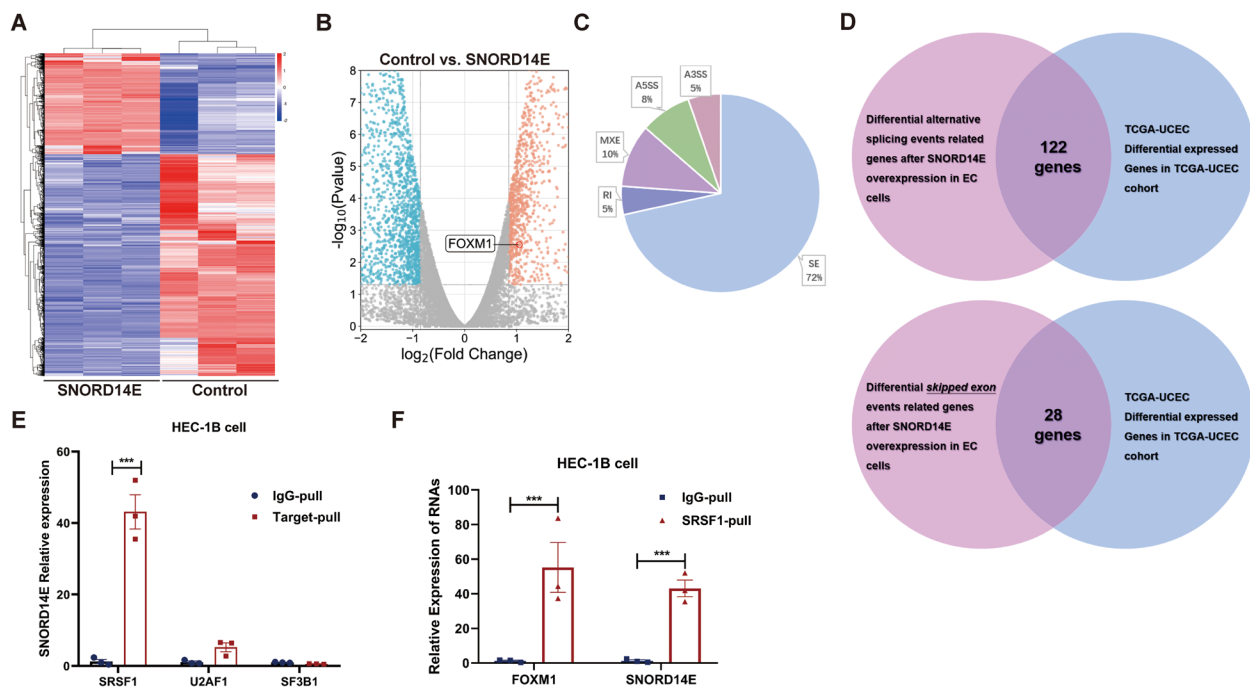


Fig. 3 SNORD14E recruits SRSF1 and affects FOXM1 alternative splicing. **A** Heatmap of differentially expressed mRNAs in RNA-seq of HEC-1B cells with or without SNORD14E overexpression. **B** Volcano plot of differentially expressed genes between SNORD14E and control. Red dots represent upregulated genes, blue dots represent downregulated genes, and gray dots represent genes that were not differentially expressed. **C** AS events following SNORD14E overexpression. SE event accounts for the most (75%). **D** Venn diagram showing significantly differential expressing genes in TCGA-UCEC cohort and differential AS events caused by SNORD14E in RNA-seq. **E** RT-qPCR of RNA immunoprecipitation (RIP) assay for detecting the enrichment of SNORD14E on AS factors SRSF1, U2AF1, and SF3B1. IgG was used as negative control. **F** RT-qPCR of the anti-SRSF1 RIP assay showed the interaction between SRSF1-SNORD14E complex and FOXM1 mRNA. * $P < 0.05$, ** $P < 0.01$, *** $P < 0.001$. Skipped exon (SE), retained intron (RI), alternative 5' splice site (A5SS), alternative 3' splice site (A3SS), mutually exclusive exon (MXE)

and migration but increased apoptosis (Fig. 5B–D). The results above indicated that SNORD14E regulated FOXM1 VIIa skipping by recruiting SRSF1, leading to increased FOXM1b and FOXM1c expression. Thus, we further explored whether FOXM1b and FOXM1c promoted the progression of EC. We constructed FOXM1b and FOXM1c plasmids, respectively, and transfected them into Ishikawa and HEC-1B cells. CCK8 analysis showed that the FOXM1b and FOXM1c transfection led to higher cell growth and migration and lower apoptosis than those in the VIIa inclusion isoform FOXM1a (Fig. 5E–G; [Supplementary Figure C](#)). In vitro studies revealed that FOXM1b and FOXM1c contributed to tumor growth in EC.

FOXM1 is a transcriptional master regulator of a number of cancers. Hence, the upregulation and activation of FOXM1 can contribute to increased cell proliferation, invasion, metastasis, and angiogenesis. FOXM1 was reported to promote β -catenin nuclear accumulation [24]. In this study, we first detected the expression of β -catenin in both the cytoplasm and the nucleus with SNORD14E overexpression or ASO targeting SNORD14E. An accumulation of β -catenin in nuclear was caused by

SNORD14E overexpression (Fig. 5H). siRNA targeting FOXM1 and siRNA targeting SRSF1 was separately transfected into cells, which decreased the total β -catenin level and the nucleus β -catenin level after FOXM1 or SRSF1 was knocked down. (Fig. 5I). We next constructed plasmids of FOXM1a, FOXM1b, and FOXM1c and transfected them into HEC-1B cells. The results showed that FOXM1b and FOXM1c overexpression led to higher β -catenin expression and nuclear accumulation than that of FOXM1a (Fig. 5J).

SNORD14E mediates FOXM1 2'-O-methylation modification to increase FOXM1 stability

2'-O-methylation modification of target RNA is the most extensive biological function of SNORDs. As RIP-PCR showed a combination between SNORD14E and the key enzyme 2'-O-methyltransferase fibrillarlin (FBL) (Fig. 6A), we next performed Nm-seq to clarify if the recognition of SNORD14E resulted in a 2'-O-methylation modification of FOXM1. Nm-seq results revealed that SNORD14E performed 2'-O-methylation modification on FOXM1 (G909), which was confirmed by RTL-P assay (Fig. 6B). Subsequently, we explored the biological effect

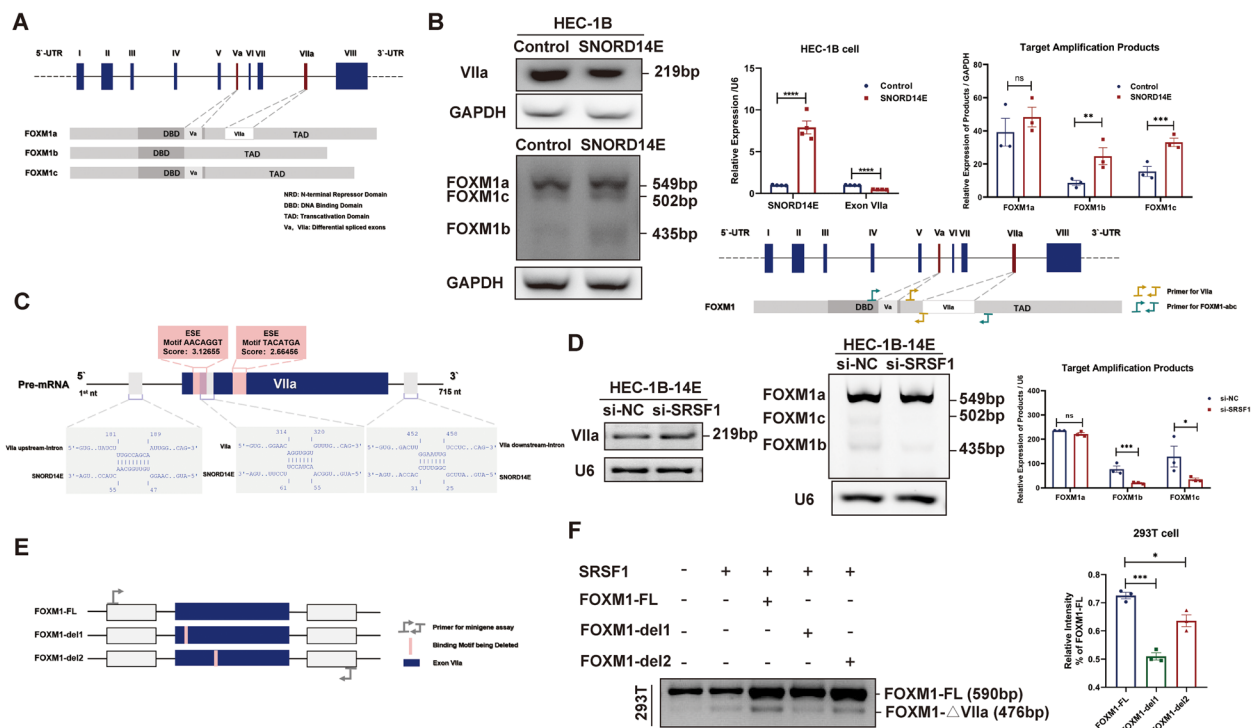


Fig. 4 SRSF1 recruited by SNORD14E recognizes exonic splicing enhancers (ESEs) on Vlla and affects FOXM1 alternative splicing. **A** Diagrams of FOXM1 transcripts and its alternative exon Va and Vlla. **B** RT-PCR validation of a selection of alternative splicing events (SE of Vlla caused by SNORD14E). **C** Prediction diagram of ESE and potential base-pair complementary region of SNORD14E. There are ESEs recognized by SRSF1 on exon Vlla, and regions potentially complementary to SNORD14E on the Vlla and flanking introns. **D** HEC-1B cells overexpressing SNORD14E were used. SNORD14E-regulated exon Vlla skip was inhibited by si-RNA targeting SRSF1, and the content of the transcripts including exon Vlla (FOXM1b and FOXM1c) were reduced by si-SRSF1. **E** Diagram of FOXM1 minigene deletion mutant plasmids. **F** Splicing analysis of FOXM1 minigene and indicated deletion mutations. The RT-PCR results are quantified and showed in histogram plots. * $P < 0.05$, ** $P < 0.01$, *** $P < 0.001$

of this modification. The Western blot analysis showed that SNORD14E promoted FOXM1 expression (Fig. 6C). After treating the SNORD14E-overexpressing cells with Act-D, we performed RT-PCR to detect the level of FOXM1 mRNA and found that the stability of FOXM1 mRNA in the SNORD14E overexpression group was significantly higher than that in the control group (Fig. 6D). We further constructed FBL-mu that inactivates the key 2'-O-methylation catalytic region of FBL and wild-type FBL-wt as control to eliminate the interference caused by the biological activity of FBL itself. Cells of SNORD14E-overexpressing were transfected with FBL-mu or FBL-wt and treated with Act-D. It showed that FBL without

the 2'-O-methylation catalysis counteracted the half-life prolongation of FOXM1 mRNA induced by SNORD14E (Fig. 6E).

SNORD14E promotes tumor growth in vivo and in PDOs

Mouse xenograft experiments were conducted to access the function of SNORD14E in EC progression. HEC-1B cells overexpressing SNORD14E and the corresponding control cells were injected into nude mice subcutaneously. SNORD14E enhanced tumor growth in vivo, as determined by the tumor growth curve (Fig. 7A–B).

EC-PDO models were established that maintained the histological and molecular features of parental EC

(See figure on next page.)

Fig. 5 SNORD14E induces β -catenin nuclear accumulation and facilitates EC progression through FOXM1 Vlla skipping. **A** Western-blot of FOXM1 and SRSF1 showing the silencing efficiency of siRNAs against FOXM1 or SRSF1. Cell proliferation (**B**) and quantification of migration and flow apoptosis assays (**C** and **D**) of siRNA targeting FOXM1 (si-FOXM1) treated HEC-1B and Ishikawa cells. **E–G** Plasmids of FOXM1a, FOXM1b and FOXM1c effects on HEC-1B cells and Ishikawa cells. **H** SNORD14E induced nuclear accumulation of β -catenin proteins in HEC-1B cells by western-blot. **I** siRNA targeting FOXM1 or SRSF1 reduced total β -catenin protein in HEC-1B and Ishikawa cells. Knockdown of FOXM1 and SRSF1 leads to a decrease content of β -catenin in the nuclear. **J** FOXM1b and FOXM1c caused more nuclear accumulation of β -catenin protein than FOXM1a

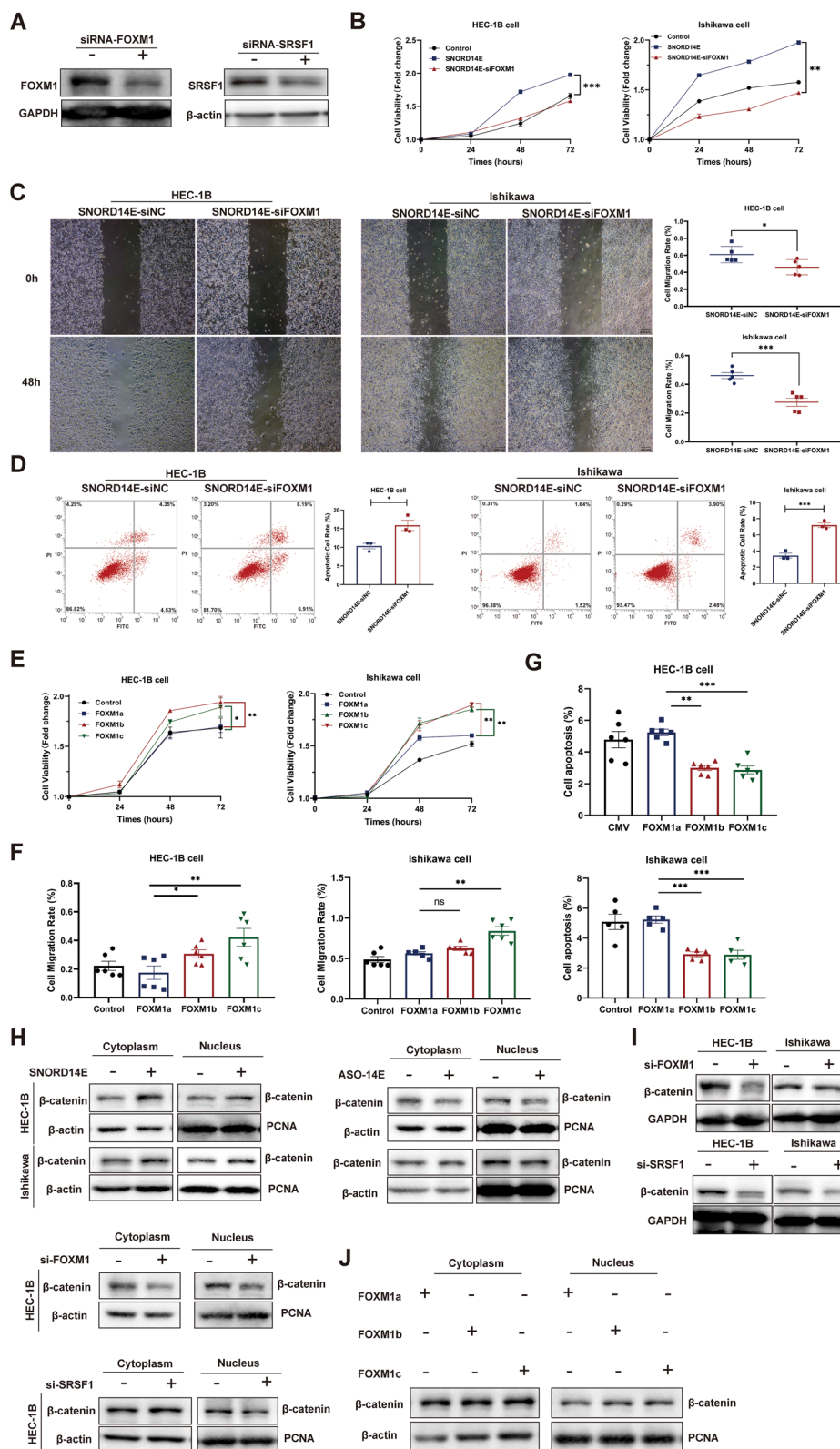


Fig. 5 (See legend on previous page.)

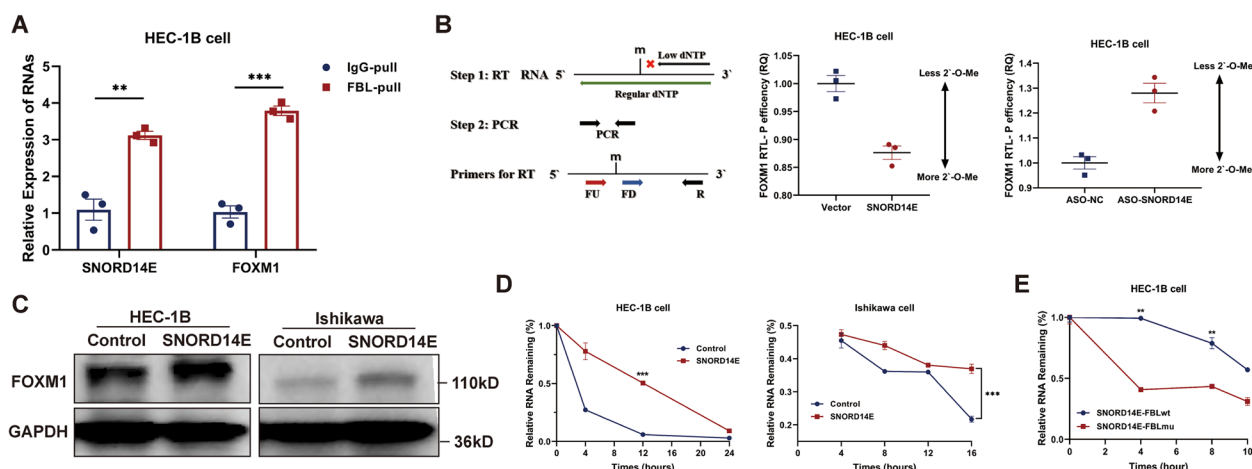


Fig. 6 SNORD14E mediates FOXM1 2'-O-methylation modification to increase FOXM1 stability. **A** RIP-PCR showed FOXM1 was enriched on SNORD14E-FBL complex. **B** The FOXM1 mRNA 2'-O-Me activities was increased after SNORD14E overexpression. **C** FOXM1 was upregulated by SNORD14E in EC cells. **D** Promotion of FOXM1 mRNA stability by SNORD14E in HEC-1B cells and Ishikawa cells. **E** FBL-wt and FBL-mu were transfected respectively into HEC-1B cells. The stability of FOXM1 mRNA is reduced by mutating the 2'-O-catalytic region of FBL (FBL-mu). ** $P < 0.01$, *** $P < 0.001$

(Fig. 7C). EC tissue was digested into 3–10-cell clusters, transfected with SNORD14E lentivirus or control lentivirus, and seeded into 3D culture media. The SNORD14E transfection resulted in a greater organoid diameter than that in the control group (Fig. 7D). Cell Counting-*Lite*[®] 3D Luminescent Cell Viability Assay was used for detecting PDO viability (Fig. 7E).

SNORD14E is a potential therapeutic target for EC

Recently, ASO drugs have been considered as therapeutic agents for EC as they are able to target RNAs more precisely than small-molecule compounds, which has been verified in vivo and in vitro. Based on the aforementioned results, we hypothesized that SNORD14E might be of value in the treatment of EC patients. First, we used ASO to knockdown the expression of SNORD14E, which significantly reduced the cell proliferation, migration, and invasion abilities, whereas the apoptosis was increased (Fig. 8A–C). Then, a xenograft mouse model was established to evaluate the therapeutic efficacy of ASO-SNORD14E treatment. A 5'-end cholesterol modification and a conventional phosphodiester-linked ASO were employed to achieve higher in vivo activity. HEC-1B and Ishikawa cells were respectively inoculated subcutaneously in nude mice, and mice with the same cells were randomly divided into two groups (ASO-NC and ASO-SNORD14E) two weeks later, when the tumor size reached 50–100 mm³. The therapeutic is presented in Fig. 8D. The tumor growth curve shows that the SNORD14E depletion by in vivo-optimized SNORD14E inhibitor (ASO-14E) application decreased the growth of the tumors in both HEC-1B and Ishikawa cell xenografts (Fig. 8E).

Encouraged by the efficacy of the selected ASO to inhibit SNORD14E and in view of the important clinical implications of such results, we generated PDO models and performed transfection-free ASO-mediated knock-down experiments in the three PDO models. The study design is shown in Fig. 8F and 8 cases of EC-PDO models were established (Fig. 8G, Supplementary Table 4). Consistent with the results obtained in the xenograft models, the growth of the PDO models in the ASO-14E group was significantly weaker than that in the control group (Fig. 8H). Collectively, the above results suggest that SNORD14E could be a potential target for EC treatment.

Discussion

Patients with advanced and recurrent EC have poor prognosis, and the 5-year survival rate is less than 20% [3]. Recognizing the patients with high-risk factors and giving them the best adjuvant therapy is therefore of critical importance to improve the management of the disease. At present, there are still deficiencies in biomolecular classifications including the initial TCGA biomolecular classification, ProMisE, TRANSPORTEC, Parra-Herran and so on, and no agreement has been reached. To find valuable therapeutic targets for patients with EC, we screened data obtained from the TCGA database and found that SNORD14E was overexpressed in EC tissues. and patients with high level of SNORD14E were distributed in the TCGA biomolecular classification subgroups without difference. These results suggest that SNORD14E may be a valuable target for prognosis independent of TCGA biomolecular classification. In

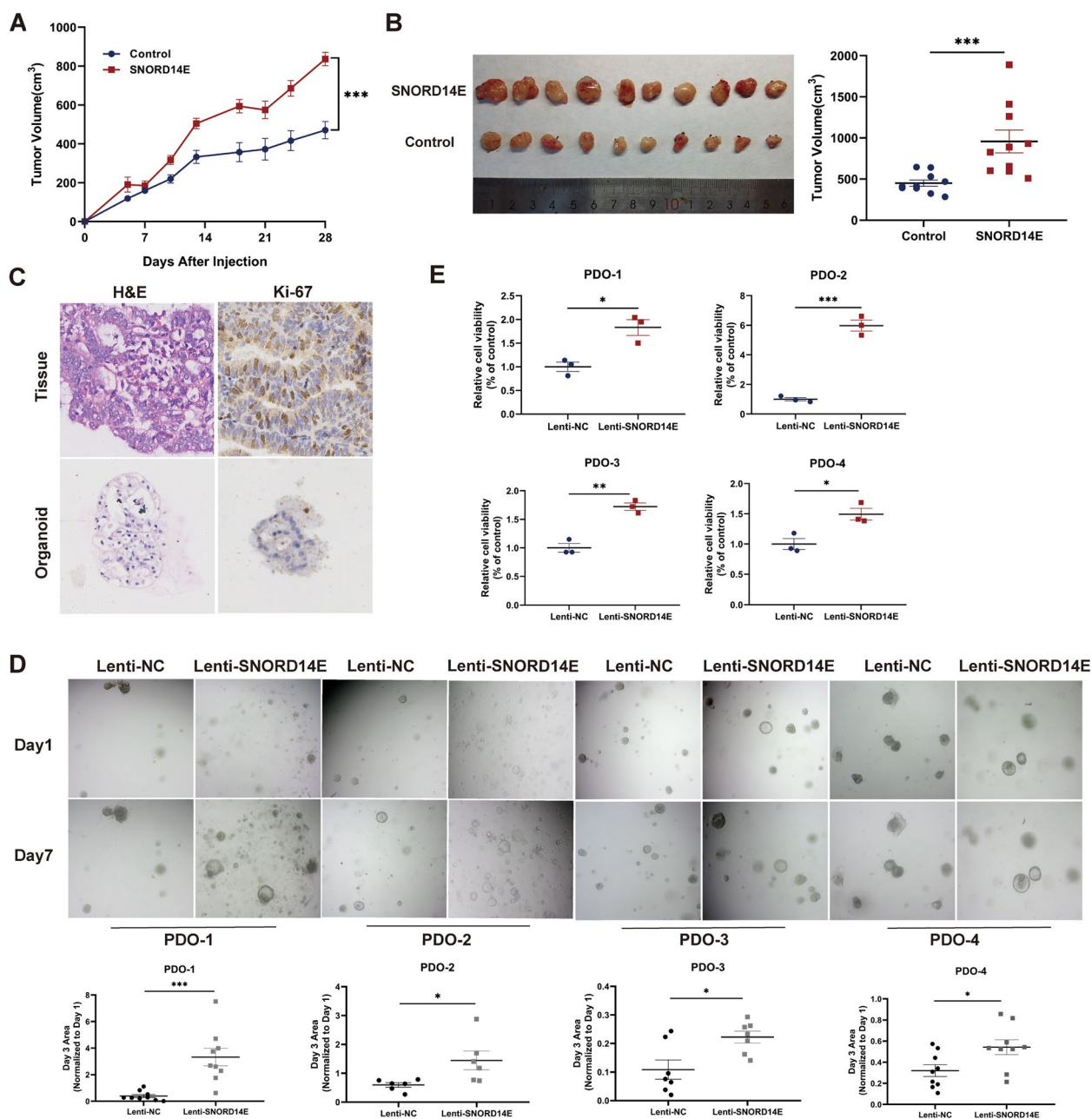


Fig. 7 SNORD14E promotes tumor growth in vivo and in PDOs. **A** Xenograft tumor growth were shown for indicated groups. HEC-1B cells were used. **B** Tumor volumes and tumor images of different groups were shown. **C** EC patients-derived organoid (EC-PDO) models were established. Represented images of IHC and HE staining were shown. **D** Images of four EC-PDO were shown and Organoids area was calculated and values were the mean \pm SD. of $n=9$ organoids. **E** Quantification of viability assays following Lentivirus transfection (Lenti-NC and Lenti-SNORD14E) treatment were shown. Cell viability assay was used for detecting affection of SNORD14E on PDO. * $P < 0.05$, ** $P < 0.01$, *** $P < 0.001$

the in vitro experiments we conducted, SNORD14E promoted the proliferation, migration, and invasion of endometrial carcinoma cells and acted as an oncogene in EC. Next, we constructed the targeted drug ASO-SNORD14E and found that ASO-SNORD14E could significantly inhibit cell proliferation and promote cell apoptosis.

TCGA-UCEC database indicated that high expression of SNORD14E caused poor prognosis in EC patients. Based on the ESMO-ESGO-ESTRO prognostic risk stratification, the proportion of patients with high level of SNORD14E in the middle-high risk group and high-risk group was more than 50%.

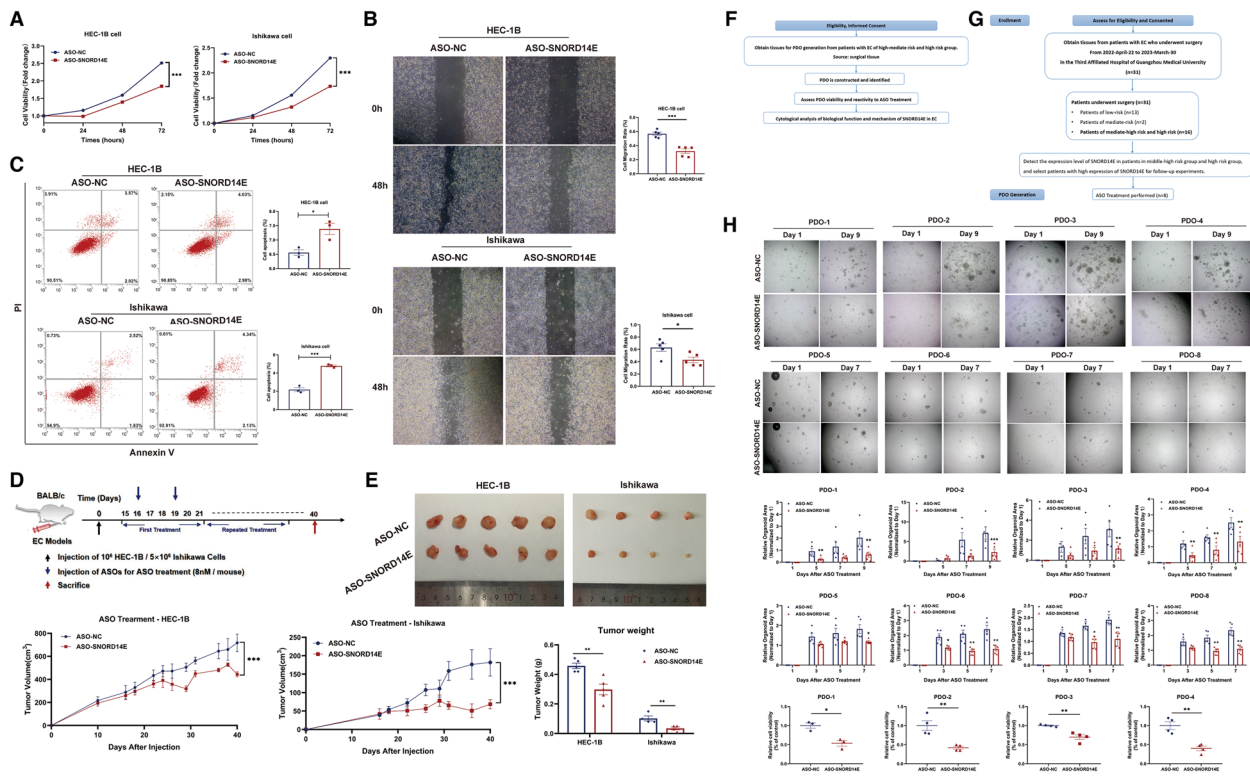


Fig. 8 SNORD14E is a potential therapeutic target for EC. **A-C** ASO targeting SNORD14E inhibited cell proliferation, migration and promoted cell apoptosis through CCK-8 assay, scratch assay and flow apoptosis assay. **D** Schematic illustration of subcutaneous injection of cells and ASO treatment on nude mice. **E** HEC-1B cell group (left) and Ishikawa cell group (right) were treated with ASO-NC or ASO-SNORD14E separately, and images of indicated groups, tumor volume and tumor weight were shown. **F** Study schema. **G** Graphical flow-chart of the study. **H** Representative images of the eight EC-PDOs treated with ASO-SNORD14E or ASO-NC and quantification of organoid size were shown. Cell viability was detected by the CellCounting-Lite 3D luminescent cell vitality and normalized with ASO-NC. * $P < 0.05$, ** $P < 0.01$, *** $P < 0.001$

In recent years, new molecular targeted therapies have achieved significant efficacy in clinical practice. Expanding the existing understanding of the molecular mechanism of EC may promote the development of effective targeted therapies and improve the overall prognosis of patients with EC. As a functional model, PDOs contain the multi omics characteristics of the original tumor and simulate the response of patients to targeted drugs, which to some extent guide clinical treatment, and are widely concerned. In the study, we successfully constructed middle-high risk and high-risk EC-PDO models and verified the therapeutic value of ASO-SNORD14E from xenograft model to preclinical PDO assay. Above all, ASO targeting SNORD14E has a therapeutic effect on EC-PDO model which derived from patients of high level of SNORD14E in the middle-high risk group and high-risk group. The results of this study provide a new option for the targeted therapy of about 50% of the patients with high expression of SNORD14E in the middle-high risk and high-risk group of EC. ASO targeting SNORD14E may be an effective treatment for EC.

To further explore the regulatory mechanism of SNORD14E, we analyzed our RNA-seq results and found that SNORD14E caused Alternative splicing events of a large number of tumor-related genes. Dysregulation of splicing events can change protein function and lead to cancer initiation and progression [25–28]. In this study, RIP-PCR results confirmed the binding of the splicing factor from the SR protein family called splice factor 1 (SRSF1) to SNORD14E. Subsequently, we screened the genes involved in AS events in the RNA-seq results, employed bioinformatics analysis, and finally focused on FOXM1 among EC-related genes because it included binding sites for SNORD14E and was enriched in SRSF1. FOXM1 has become an oncoprotein and a powerful biomarker of poor prognosis for many human malignancies in recent studies [29]. The upregulation and activation of FOXM1 can lead to a variety of tumor-associated phenotypes such as cell proliferation, tumor stem cells, drug resistance, invasion, metastasis, and angiogenesis [30–33], which have been reported as top-level gene expression biomarkers with poor prognosis [34]. The

high FOXM1 expression in endometrial carcinoma is closely associated with the prognosis, pathological stage, and clinical grade of endometrial carcinoma patients [35] and can thus serve as a marker of endometrial carcinoma prognosis and a candidate target for its treatment [36]. The FOXM1 gene comprises ten exons, including exons I-VIII and the alternatively spliced exons Va and VIIa [37–39]. Based on the AS of exons Va and VIIa, three FOXM1 subtypes can be classified: FOXM1a including all ten exons, FOXM1b with lacking alternative exons Va and VIIa, and FOXM1c including the alternative exon Va but lacking the alternative exon VIIa [39, 40]. Our results indicate that the overexpression of SNORD14E promotes the exon VIIa skipping of FOXM1, resulting in an increase in the transcript FOXM1b and FOXM1c subtypes.

AS is characterized by the ability to accurately identify and splice the correct splice sites among numerous potential splice sites [41]. The proper recognition of the splice sites is ensured by high degrees of matching to the consensus sequences or by the assistance of cis-acting elements and trans-acting factors [42, 43]. Reportedly, exon skipping may be affected by cis-acting elements such as exon splice enhancers (ESEs) [23, 42]. Studies have shown that SRSF1 usually binds to ESEs to promote splicing [23]. The AS event mediated by SRSF1 and the carcinogenic effects of SRSF1 have been observed in several tumors [44–46]. For example, the splice switch of MYO1B directly regulated by SRSF1 increased the carcinogenic potential of glioma cells through the PDK1/AKT and PAK/LIMK pathways [47]. Next, to explore the effect of SNORD14E on the exon skipping of FOXM1 VIIa, we predicted the ESEs element located on THE alternative exon VIIa using the splice site prediction program ESE Finder (<http://exon.cshl.edu/ESE/>) [48, 49], suggesting that two potential ESE elements on the alternative exon VIIa might bind to SRSF1. We found that SRSF1 always led to the exclusion of the optional exon VIIa of FOXM1, which was more pronounced in cells with SNORD14E overexpression. The effect of SNORD14E on the FOXM1 exon VIIa skipping was rescued by knocking down SRSF1 in endometrial carcinoma cell lines, suggesting that SNORD14E recognized FOXM1 and promoted the FOXM1 exon VIIa skipping by recruiting SRSF1 in combination with SRSF1. Minigene analysis showed that the enrichment of the SRSF1-binding motif within exon VIIa resulted in exon VIIa skipping, whereas SNORD14E was able to facilitate this process by recruiting SRSF1.

Of note, the assessment of the functional characteristics indicates that FOXM1b and FOXM1c are transcriptionally active, whereas FOXM1a is not [50–53]. Both FOXM1b and FOXM1c can promote malignant behavior of tumors, of which, FOXM1c may promote

a proliferation and metastasis phenotype, whereas FOXM1b induces more pronouncedly a migration and invasion phenotype [54]. After the plasmids of three FOXM1 subtypes were constructed and tested in vitro, in contrast to FOXM1a, FOXM1b and FOXM1c were found to be able to promote the proliferation and migration of EC cells and inhibit apoptosis. However, after the transfection of siRNA to knock down FOXM1, the pro-cancer effect of SNORD14E on EC cells was almost completely offset.

Recent snoRNA research has been focused mainly on the 2'-O-methylation modification function. That is, C/D box snoRNA performs 2'-O-methylation modification in a variety of RNAs, including mRNA, through base complementary pairing and is involved in gene regulation [55, 56]. Nm (2'-O-methylation, where N represents any nucleotide) is one of the most common and widely distributed RNA post-transcriptional modifications in RNA. Some of these modifications are directed by box C/D snoRNAs and catalyzed by FBL [57]. Using RIP detection, we found that SNORD14E was connected to FBL, indicating that SNORD14E might have a Nm modification. Nm-seq results suggested that SNORD14E was capable of NM modification of multiple genes, including FOXM1. RTL-P assay confirmed the Nm modification of FOXM1 caused by SNORD14E. Notably, the Nm modification prolonged the half-life of FOXM1 mRNA and inhibited the protein degradation of FOXM1. We further mutated FBL as the domain of the key enzyme for 2'-O-methylation modification and found that, relative to FBL-wt, FBL-mu without the 2'-O-methylation modification could not affect the degradation of FOXM1 mRNA and protein, *i.e.*, the effect of SNORD14E on mRNA and protein levels of FOXM1 was achieved after Nm modification.

β -catenin is involved in a range of tumor-related signaling pathways and is tightly regulated at three levels: protein stability, subcellular localization, and transcriptional activity [58, 59]. FOXM1 enhances the nuclear localization of β -catenin and the expression of downstream target genes by binding to β -catenin to promote the occurrence and development of a variety of tumors. In gliomas, FOXM1 promotes tumorigenesis by direct interaction with β -catenin and acts as a cofactor for β -catenin stabilization [24]. However, the effects of the interactions between FOXM1 and β -catenin in EC have not been elucidated. In this study, we discovered that SNORD14E promoted the nuclear aggregation of β -catenin which was inhibited after the knockdown of FOXM1. In the analysis of the effect of SNORD14E on alternative FOXM1 splicing, we found that the knockdown of SRSF1 also inhibited the nuclear aggregation of β -catenin. Further, we performed analyses to determine the nuclear content of β -catenin after the overexpression of FOXM1a,

FOXM1b, and FOXM1c, respectively. We established that both FOXM1b and FOXM1c promoted more the nuclear aggregation of β -catenin than FOXM1a. The aforementioned results indicated that SNORD14E could promote the nuclear aggregation of β -catenin through multi-faceted regulation of FOXM1, thus promoting the occurrence and development of endometrial carcinoma.

Conclusions

In this study, we found that SNORD14E is highly expressed in EC and reduces DFS and RFS of patients with EC. SNORD14E can promote the malignant phenotype of EC cells. We further clarified the mechanism of SNORD14E in EC, and confirmed the application prospect of ASO drugs targeting SNORD14E in patients with middle-high risk and high-risk prognostic factors of EC.

Limitations

This study is a preclinical research based on PDOs. PDOs can better simulate the characteristics of molecular properties and tumor heterogeneity of parental tumor tissues. They are suitable models for preclinical research of drugs and closer to the true reflection of patients on drugs. Nevertheless, the results of preclinical research need to go through procedures including pharmacology, pharmacokinetics, toxicology, long-term toxicity tests and phase I-III trials of clinical research before they can be finally applied to patients. There is still a long way to go from this study to clinical application.

Abbreviations

TCGA	The Cancer Genome Atlas
PDO	Patient-derived organoid
qRT-PCR	Real-time quantitative reverse transcription-polymerase chain reaction
RIP	RNA immunoprecipitation
AS	Alternative splicing
ASO	Antisense oligonucleotide
IHC	Immunohistochemistry
IF	Immunofluorescence
Nm-seq	2'-O-Methylation Modification sequencing
RTL-P	Reverse Transcription at Low deoxy-ribonucleoside triphosphate concentrations followed by PCR

Supplementary Information

The online version contains supplementary material available at <https://doi.org/10.1186/s13046-023-02801-2>.

Additional file 1: Supplementary Figure A. There were binding region between SNORD14E and MELK and CCDC150. **Supplementary Figure B.** The mRNAs of MELK and CCDC150 were not enriched on SRSF1. **Supplementary Figure C.** FOXM1b and FOXM1c promoted cell migration and inhibited cell apoptosis comparing with FOXM1a and Control.

Additional file 2: Supplementary Table 1. Primer sequences used for PCR assays. **Supplementary Table 2.** Primer sequences used for RTL-P assays. **Supplementary Table 3.** The oligonucleotides used in this study. **Supplementary Table 4.** Patient clinical characteristic for the patient-derived cancer organoids.

Additional file 3: Supplementary Table 5. The full sequence of different isoforms of FOXM1.

Additional file 4: Supplementary Table 6. Sequences of plasmids constructed for minigene assay.

Acknowledgements

We are very grateful to the Cancer Genome Atlas (TCGA) database for providing the transcriptome and clinical information. We thank Shanghai NewCore Biotechnology Co., Ltd. (<https://www.bioinformatics.com.cn>) for providing visualization support.

Authors' contributions

YZ developed the concept and provided overall direction. XC designed and conducted the experiments, wrote the manuscript. XC, XL, QHL and BFL analyzed data and conducted the cell and mice experiments. XC, BMX and YMJ collected data, constructed PDO models and contributed to the data analysis and interpretation. All authors have read and approved the submitted version.

Funding

This work was supported by the National Nature Science Foundation of China, CHN (No. 82072854; 82272985); Natural Science Foundation of Guangdong Province (No. 2022A1515012293); the Project for Key Medicine Discipline Construction of Guangzhou Municipality, CHN (No. 2021–2023-17); Science and Technology Projects in Guangzhou (No. 202201020093).

Availability of data and materials

The resources, tools and codes used in our analyses were described in each method section in the methods. For any further of the data requests, please contact the corresponding author. The public datasets of TCGA analysed during the current study is: TCGA-UCEC <https://portal.gdc.cancer.gov/projects/TCGA-UCEC>.

Declarations

Ethics approval and consent to participate

All the use of human tissue were approved by the Ethics Committee of Guangzhou Medical University (No. 2020–066). Informed consent was obtained from all patients. The Ethics Committee of Guangdong Medical Laboratory Animal Center approved the use of experimental animals in this study (No. B202008-10).

Consent for publication

Not applicable.

Competing interests

The authors declare that they have no competing interests.

Author details

¹Department of Obstetrics and Gynecology, Department of Gynecologic Oncology Research Office, Guangzhou Key Laboratory of Targeted Therapy for Gynecologic Oncology, Guangdong Provincial Key Laboratory of Major Obstetric Diseases, The Third Affiliated Hospital of Guangzhou Medical University, No.63 Duobao Road, Liwan District, Guangzhou 510150, Guangdong Province, PR China.

Received: 13 March 2023 Accepted: 16 August 2023

Published online: 05 September 2023

References

1. Ayhan A, Taskiran C, Celik C, Guney I, Yuce K, Ozyar E, et al. Is there a survival benefit to adjuvant radiotherapy in high-risk surgical stage I endometrial cancer? *Gynecol Oncol*. 2002;86(3):259–63.
2. Gottwald L, Pluta P, Piekarski J, Szych M, Hendzel K, Topczewska-Tylińska K, et al. Long-term survival of endometrioid endometrial cancer patients. *Arch Med Sci : AMS*. 2010;6(6):937–44.
3. Colombo N, Creutzberg C, Amant F, Bosse T, González-Martín A, Ledermann J, et al. ESMO-ESGO-ESTRO Consensus Conference on Endometrial

- Cancer: Diagnosis, Treatment and Follow-up. *Int J Gynecol Cancer*. 2016;26(1):2–30.
4. Creutzberg CL, van Putten WL, Koper PC, Lybeert ML, Jobsen JJ, Wárlám-Rodenhuis CC, et al. Surgery and postoperative radiotherapy versus surgery alone for patients with stage-1 endometrial carcinoma: multicentre randomised trial. PORTEC study group. *Post operative radiation therapy in endometrial carcinoma*. *Lancet (London, England)*. 2000;355(9213):1404–11.
 5. Keys HM, Roberts JA, Brunetto VL, Zaino RJ, Spirtos NM, Bloss JD, et al. A phase III trial of surgery with or without adjunctive external pelvic radiation therapy in intermediate risk endometrial adenocarcinoma: a Gynecologic Oncology Group study. *Gynecol Oncol*. 2004;92(3):744–51.
 6. Kandath C, Schultz N, Cherniack AD, Akbani R, Liu Y, Shen H, et al. Integrated genomic characterization of endometrial carcinoma. *Nature*. 2013;497(7447):67–73.
 7. Talhouk A, McConechy MK, Leung S, Yang W, Lum A, Senz J, et al. Confirmation of ProMisE: A simple, genomics-based clinical classifier for endometrial cancer. *Cancer*. 2017;123(5):802–13.
 8. Stelloo E, Nout RA, Osse EM, Jürgenliemk-Schulz IJ, Jobsen JJ, Lutgens LC, et al. Improved risk assessment by integrating molecular and clinicopathological factors in early-stage endometrial cancer-combined analysis of the PORTEC cohorts. *Clin Cancer Res*. 2016;22(16):4215–24.
 9. Kommos FK, Karnezis AN, Kommos F, Talhouk A, Taran FA, Staebler A, et al. L1CAM further stratifies endometrial carcinoma patients with no specific molecular risk profile. *Br J Cancer*. 2018;119(4):480–6.
 10. Yamazaki S, Ohka F, Hirano M, Shiraki Y, Motomura K, Tanahashi K, et al. Newly established patient-derived organoid model of intracranial meningioma. *Neuro Oncol*. 2021;23(11):1936–48.
 11. Semertzidou A, Brosens JJ, McNeish I, Kyrgiou M. Organoid models in gynaecological oncology research. *Cancer Treat Rev*. 2020;90:102103.
 12. Boretto M, Maenhoudt N, Luo X, Hennes A, Boeckx B, Bui B, et al. Patient-derived organoids from endometrial disease capture clinical heterogeneity and are amenable to drug screening. *Nat Cell Biol*. 2019;21(8):1041–51.
 13. Boretto M, Cox B, Noben M, Hendriks N, Fassbender A, Roose J, et al. Development of organoids from mouse and human endometrium showing endometrial epithelium physiology and long-term expandability. *Development (Cambridge, England)*. 2017;144(10):1775–86.
 14. Chen S, Li QH, Chen X, Bao HJ, Wu W, Shen F, et al. SNORA70E promotes the occurrence and development of ovarian cancer through pseudouridylation modification of RAP1B and alternative splicing of PARPBP. *J Cell Mol Med*. 2022;26(20):5150–64.
 15. Dai Q, Moshitch-Moshkovitz S, Han D, Kol N, Amariglio N, Rechavi G, et al. Nm-seq maps 2'-O-methylation sites in human mRNA with base precision. *Nat Methods*. 2017;14(7):695–8.
 16. Cancer Genome Atlas Research Network. Integrated genomic analyses of ovarian carcinoma. *Nature*. 2011;474(7353):609–15.
 17. Tefferi A, Finke CM, Lasho TL, Hanson CA, Ketterling RP, Gangat N, et al. U2AF1 mutation types in primary myelofibrosis: phenotypic and prognostic distinctions. *Leukemia*. 2018;32(10):2274–8.
 18. Furney SJ, Pedersen M, Gentien D, Dumont AG, Rapinat A, Desjardins L, et al. SF3B1 mutations are associated with alternative splicing in uveal melanoma. *Cancer Discov*. 2013;3(10):1122–9.
 19. Anczuków O, Akerman M, Cléry A, Wu J, Shen C, Shirole NH, et al. SRSF1-Regulated Alternative Splicing in Breast Cancer. *Mol Cell*. 2015;60(1):105–17.
 20. Ni J, Tien AL, Fournier MJ. Small nucleolar RNAs direct site-specific synthesis of pseudouridine in ribosomal RNA. *Cell*. 1997;89(4):565–73.
 21. Cáceres JF, Kornblihtt AR. Alternative splicing: multiple control mechanisms and involvement in human disease. *Trends in genetics : TIG*. 2002;18(4):186–93.
 22. Hastings ML, Krainer AR. Pre-mRNA splicing in the new millennium. *Curr Opin Cell Biol*. 2001;13(3):302–9.
 23. Cartegni L, Chew SL, Krainer AR. Listening to silence and understanding nonsense: exonic mutations that affect splicing. *Nat Rev Genet*. 2002;3(4):285–98.
 24. Zhang N, Wei P, Gong A, Chiu WT, Lee HT, Colman H, et al. FoxM1 promotes β -catenin nuclear localization and controls Wnt target-gene expression and glioma tumorigenesis. *Cancer Cell*. 2011;20(4):427–42.
 25. Bechara EG, Sebestyén E, Bernardis I, Eyra E, Valcárcel J. RBM5, 6, and 10 differentially regulate NUMB alternative splicing to control cancer cell proliferation. *Mol Cell*. 2013;52(5):720–33.
 26. Shkreta L, Bell B, Revil T, Venables JP, Prinos P, Elela SA, et al. Cancer-Associated Perturbations in Alternative Pre-messenger RNA Splicing. *Cancer Treat Res*. 2013;158:41–94.
 27. David CJ, Manley JL. Alternative pre-mRNA splicing regulation in cancer: pathways and programs unhinged. *Genes Dev*. 2010;24(21):2343–64.
 28. Venables JP. Aberrant and alternative splicing in cancer. *Can Res*. 2004;64(21):7647–54.
 29. Liu C, Barger CJ, Karpf AR. FOXM1: a multifunctional oncoprotein and emerging therapeutic target in ovarian cancer. *Cancers*. 2021;13(12):3065.
 30. Lam EW, Brosens JJ, Gomes AR, Koo CY. Forkhead box proteins: tuning forks for transcriptional harmony. *Nat Rev Cancer*. 2013;13(7):482–95.
 31. Raychaudhuri P, Park HJ. FoxM1: a master regulator of tumor metastasis. *Can Res*. 2011;71(13):4329–33.
 32. Halasi M, Gartel AL. FOX(M1) news—it is cancer. *Mol Cancer Ther*. 2013;12(3):245–54.
 33. Alvarez-Fernández M, Medema RH. Novel functions of FoxM1: from molecular mechanisms to cancer therapy. *Front Oncol*. 2013;3:30.
 34. Gentles AJ, Newman AM, Liu CL, Bratman SV, Feng W, Kim D, et al. The prognostic landscape of genes and infiltrating immune cells across human cancers. *Nat Med*. 2015;21(8):938–45.
 35. Feng Y, Li S, Zhang R, Liu F, Xu Q, Ding H, et al. FOXM1 as a prognostic biomarker promotes endometrial cancer progression via transactivation of SLC27A2 expression. *Int J Clin Exp Pathol*. 2018;11(8):3846–57.
 36. Bosquet JG, Zhang Q, Cliby WA, Bakkum-Gamez JN, Cen L, Dowdy SC, et al. Association of a novel endometrial cancer biomarker panel with prognostic risk, platinum insensitivity, and targetable therapeutic options. *PLoS ONE*. 2021;16(1):e0245664.
 37. Yao KM, Sha M, Lu Z, Wong GG. Molecular analysis of a novel winged helix protein, WIN. Expression pattern, DNA binding property, and alternative splicing within the DNA binding domain. *J Biol Chem*. 1997;272(32):19827–36.
 38. Korver W, Roose J, Heinen K, Weghuis DO, de Bruijn D, van Kessel AG, et al. The human TRIDENT/HFH-11/FKHL16 gene: structure, localization, and promoter characterization. *Genomics*. 1997;46(3):435–42.
 39. Laoukili J, Stahl M, Medema RH. FoxM1: at the crossroads of ageing and cancer. *Biochem Biophys Acta*. 2007;1775(1):92–102.
 40. Ye H, Kelly TF, Samadani U, Lim L, Rubio S, Overdier DG, et al. Hepatocyte nuclear factor 3/fork head homolog 11 is expressed in proliferating epithelial and mesenchymal cells of embryonic and adult tissues. *Mol Cell Biol*. 1997;17(3):1626–41.
 41. Srebrow A, Kornblihtt AR. The connection between splicing and cancer. *J Cell Sci*. 2006;119(Pt 13):2635–41.
 42. Bonnal SC, López-Oreja I, Valcárcel J. Roles and mechanisms of alternative splicing in cancer - implications for care. *Nat Rev Clin Oncol*. 2020;17(8):457–74.
 43. Lopez AJ. Alternative splicing of pre-mRNA: developmental consequences and mechanisms of regulation. *Annu Rev Genet*. 1998;32:279–305.
 44. de Miguel FJ, Sharma RD, Pajares MJ, Montuenga LM, Rubio A, Pio R. Identification of alternative splicing events regulated by the oncogenic factor SRSF1 in lung cancer. *Can Res*. 2014;74(4):1105–15.
 45. Comiskey DF Jr, Jacob AG, Singh RK, Tapia-Santos AS, Chandler DS. Splicing factor SRSF1 negatively regulates alternative splicing of MDM2 under damage. *Nucleic Acids Res*. 2015;43(8):4202–18.
 46. Sheng J, Zhao J, Xu Q, Wang L, Zhang W, Zhang Y. Bioinformatics analysis of SRSF1-controlled gene networks in colorectal cancer. *Oncol Lett*. 2017;14(5):5393–9.
 47. Liang J, Wen J, Huang Z, Chen XP, Zhang BX, Chu L. Small Nucleolar RNAs: Insight Into Their Function in Cancer. *Front Oncol*. 2019;9:587.
 48. Smith PJ, Zhang C, Wang J, Chew SL, Zhang MQ, Krainer AR. An increased specificity score matrix for the prediction of SF2/ASF-specific exonic splicing enhancers. *Hum Mol Genet*. 2006;15(16):2490–508.
 49. Cartegni L, Wang J, Zhu Z, Zhang MQ, Krainer AR. ESEfinder: A web resource to identify exonic splicing enhancers. *Nucleic Acids Res*. 2003;31(13):3568–71.
 50. Korver W, Roose J, Clevers H. The winged-helix transcription factor Trident is expressed in cycling cells. *Nucleic Acids Res*. 1997;25(9):1715–9.
 51. Liao GB, Li XZ, Zeng S, Liu C, Yang SM, Yang L, et al. Regulation of the master regulator FOXM1 in cancer. *Cell Commun Signal*. 2018;16(1):57.
 52. Zhang X, Zhang L, Du Y, Zheng H, Zhang P, Sun Y, et al. A novel FOXM1 isoform, FOXM1D, promotes epithelial-mesenchymal transition and

- metastasis through ROCKs activation in colorectal cancer. *Oncogene*. 2017;36(6):807–19.
53. Gartel AL. FOXM1 in Cancer: Interactions and Vulnerabilities. *Can Res*. 2017;77(12):3135–9.
54. Lam AK, Ngan AW, Leung MH, Kwok DC, Liu VW, Chan DW, et al. FOXM1b, which is present at elevated levels in cancer cells, has a greater transforming potential than FOXM1c. *Front Oncol*. 2013;3:11.
55. Falaleeva M, Welden JR, Duncan MJ, Stamm S. C/D-box snoRNAs form methylating and non-methylating ribonucleoprotein complexes: Old dogs show new tricks. *BioEssays*. 2017;39(6):1600264.
56. Barros-Silva D, Klavert J, Jenster G, Jerónimo C, Lafontaine DLJ, Martens-Uzunova ES. The role of OncoSnoRNAs and Ribosomal RNA 2'-O-methylation in Cancer. *RNA Biol*. 2021;18(sup1):61–74.
57. Byszewska M, Śmiateński M, Purta E, Bujnicki JM. RNA methyltransferases involved in 5' cap biosynthesis. *RNA Biol*. 2014;11(12):1597–607.
58. White BD, Chien AJ, Dawson DW. Dysregulation of Wnt/ β -catenin signaling in gastrointestinal cancers. *Gastroenterology*. 2012;142(2):219–32.
59. Bosco EE, Nakai Y, Hennigan RF, Ratner N, Zheng Y. NF2-deficient cells depend on the Rac1-canonical Wnt signaling pathway to promote the loss of contact inhibition of proliferation. *Oncogene*. 2010;29(17):2540–9.

Publisher's Note

Springer Nature remains neutral with regard to jurisdictional claims in published maps and institutional affiliations.

Ready to submit your research? Choose BMC and benefit from:

- fast, convenient online submission
- thorough peer review by experienced researchers in your field
- rapid publication on acceptance
- support for research data, including large and complex data types
- gold Open Access which fosters wider collaboration and increased citations
- maximum visibility for your research: over 100M website views per year

At BMC, research is always in progress.

Learn more biomedcentral.com/submissions

